

# Decision-rule-based Pipeline to Detect Overhead Power Lines and Vegetation Contact Areas Using Mobile LiDAR Data in Brazilian Urban Regions

Renan Américo Ribeiro de Oliveira<sup>1</sup>, Mauricio Galo<sup>1,2</sup>

<sup>1</sup>Graduate Program in Cartographic Sciences, São Paulo State University (UNESP),  
Presidente Prudente, São Paulo, Brazil - renan.americo@unesp.br

<sup>2</sup>Department of Cartography, Faculty of Sciences and Technology (FCT), São Paulo State University (UNESP),  
Presidente Prudente, São Paulo, Brazil - mauricio.galo@unesp.br

**Keywords:** LiDAR Data, Power distribution lines, Vegetation management, Automatic data annotation, Hough Transform, Geometric tensors

## Abstract

Vegetation encroachment is a major issue to the reliability of overhead power distribution networks, particularly in Brazilian urban areas where networks maintenance is still largely manual and the management uses the reactive approach instead of proactive solutions. This paper presents a decision-rule-based pipeline designed to automatically detect overhead power lines and vegetation contact areas using high-density mobile LiDAR data in Brazilian urban environments. The proposed method classifies point clouds into four primary classes: low-voltage cables, medium-voltage cables, poles, and trees in proximity to the power distribution network systems. The pipeline leverages geometric features derived from eigenvalue-based tensor analysis, height and density filters, Hough Transform, and region-growing techniques, to effectively segment and classify electric components and surrounding vegetation. The method was tested in two distinct urban scenarios, including suburban and downtown areas in Presidente Prudente, São Paulo, Brazil, with point densities exceeding 2 million points per square meter. Evaluation against reference datasets from a utility company demonstrated high precision and F-scores above 0.85 for power lines detection. Despite limitations related to parameter tuning, leak of reference data for tree detection evaluation, the pipeline offers a promising approach for semi-automatic annotation of LiDAR datasets. This process can support future applications in deep learning model training for urban asset monitoring and vegetation management. It is suggested that future works focus on reducing parameter dependency and enhancing vegetation classification reliability.

## 1. Introduction

Electricity is essential to modern society and plays a critical role in human well-being, whether in everyday activities or economic development. In Brazil, according to the National Electric Energy Agency (ANEEL - Agência Nacional de Energia Elétrica, 2021), electricity reaches the majority of the population — approximately 208 million people — through power distribution networks systems. These systems, installed and maintained by utility companies, are predominantly composed of overhead metallic conductor cables, poles, crossarms, and other equipment operating at low and medium voltage levels.

Given the vulnerability of these networks — especially due to their exposure and use of uninsulated conductors, as the power lines — continuous and efficient monitoring becomes a strategic and relevant demand, particularly in the context of accelerating climate changes. The increasing frequency of extreme weather events, such as strong tropical storms and severe winds, poses significant risks and are leading to widespread outages in Brazilian cities. This monitoring enables utilities to detect structural faults and environmental risks early, particularly those associated with interactions between power lines and urban vegetation. Monitoring must cover both the condition of power lines components and surrounding objects, especially vegetation, since trees and bushes growing close to lines can cause damage, outages, or even fire (Matikainen et al., 2016).

Vegetation management inspection and monitoring are essential for maintaining the reliability and continuity of power

distribution (Bergmann et al., 2024), and there are several techniques for this task in the literature (Carvalho et al., 2018). However, traditionally in Brazil, such tasks have been conducted manually, involving in-person inspections that are labor intensive, time-consuming, and prone to human error. Furthermore, utility companies still largely rely on these manual inspections and vary significantly in their operational practices to address this issue, due to the fragmented nature of regional concessions (de Oliveira, 2022). Consequently, there is a lack of standardization and coordination in dealing with vegetation-related disruptions.

This fragmented landscape complicates the development of cohesive strategies for vegetation control and emphasizes the need for scalable, technology-driven solutions. Despite being a well-known concern among utilities companies, most companies still operate under a reactive framework — intervening only after service failures occur — which is dominated as a corrective mitigation measure. On the other hand, preventive measures are not only more cost-effective but also enhance the quality and continuity of electricity supply to the population, especially in large urban centers. Recent studies have shown that implementing vegetation management standards focused on preventive trimming can reduce outage rates by up to 48%, highlighting the greater effectiveness of proactive measures compared to reactive interventions (Cerrai et al., 2019).

However, for preventive strategies to be effective, utility companies require up-to-date and accurate inventories of urban vegetation and electrical infrastructure components. These can be developed through automated urban inventories powered

by remote sensing and intelligent data processing methods, thereby reducing reliance on emergency interventions. Although different types of information can be used, a technological approach to support the creation of such inventories is the use of LiDAR (Light Detection and Ranging) data. LiDAR systems generate high-resolution 3D point clouds that offer detailed spatial information about both vegetation and power infrastructure (Chen et al., 2018; de Oliveira, 2022).

There are several types of LiDAR systems: Airborne Laser Scanning (ALS), Terrestrial Laser Scanning (TLS), Mobile Laser Scanning (MLS) and Wearable Laser Scanning (WLS), each with unique characteristics. The MLS systems are particularly well-suited for urban environments due to their ability to capture very accurate, high-density point clouds — often a few thousand points per square meter — while being deployed on moving platforms through complex cityscapes (Wang et al., 2019). Among the applications for point clouds obtained in urban regions from LiDAR data, some include roof detection (dos Santos et al., 2022), historical building monitoring (Zhang et al., 2024), vegetation identification (Alencar et al., 2023), urban scene mapping with autonomous vehicles (Alaba and Ball, 2022), infrastructure railway environments modeling (Zhu and Hyyppä, 2014) and WLS devices (Zou et al., 2025), in addition to identification of power distribution networks (de Oliveira, 2022; Bergmann et al., 2024).

Aiming to identify those networks and also transmission lines, most of the existing studies employ methods based on decision-rule algorithms or classifiers structured using machine learning algorithms (Munir et al., 2023). With the popularization of pre-trained machine learning models and the advancement in modern computational processing capabilities, methods have increasingly shifted toward the use of artificial intelligence, incorporating progressively more complex models. An example of this trend is the adoption of panoptic segmentation approaches, which essentially combine semantic and instance classification in LiDAR data using deep learning techniques (Xiang et al., 2023).

In contrast to deep learning approaches that require extensive annotated data, clustering-based methods have also been employed to segment MLS data in urban scenes, such as density-based clustering strategies tailored to extract structural elements from large-scale point clouds (Li et al., 2017). Similarly, Lehtomäki et al. (2019) developed an automatic power line extraction algorithm using MLS, achieving high precision in rural environments with this kind of algorithm.

Given the challenges faced by Brazilian utility companies in managing vegetation and infrastructure assets, combined with the limitations of directly applying deep learning methods to MLS point clouds segmentation such as limited accuracy and the high cost of manual data annotation in terms of time and human labor (Wang et al., 2024), the integration of decision-rule-based methods to initially annotate LiDAR training data emerges as a promising strategy to enhance the productivity and scalability of deep learning models. These methods, as employed by Oliveira (2022), that used high-precision MLS data, can serve as an efficient pre-processing step by providing structured and interpretable initial classifications. These preliminary classifications can significantly reduce the volume of manual annotation required for deep learning training datasets, which remains one of the most time-consuming and resource-intensive phases in the development of robust neural networks (Bergmann et al., 2024) to segment MLS Data. By

leveraging the deterministic nature of decision-rules, researchers can generate high-confidence pseudo-labels to bootstrap deep learning models, ultimately accelerating model convergence and improving scalability for large-scale urban inventories.

This work proposes a decision-rule-based algorithm designed to identify and classify MLS data into four predefined classes: low-voltage (LV) cables, medium-voltage (MV) cables, poles and vegetation near these electric components. This classification is based on geometric features derived from tensors constructed using eigenvalues estimated within 3D neighborhoods of each MLS point cloud. Additionally, the method incorporates point density estimation, Hough Transform and region growing techniques to characterize, segment and filter the data in a sequential processing pipeline.

## 2. Methods

### 2.1 Test area

The test area for development and evaluation of the decision-rule-based algorithm proposed was carried out in the city of Presidente Prudente, São Paulo, Brazil. Two distinct urban regions with 62500 m<sup>2</sup> were selected for testing: the first is a suburban area characterized primarily by residential houses (Figure 1a), while the second is located in the downtown area (Figure 1b), featuring taller buildings and more complex scenarios.

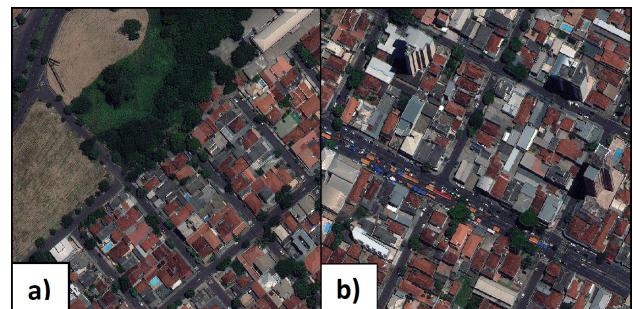


Figure 1. Low (a) and high (b) density urban areas, Presidente Prudente, São Paulo, Brazil.

The dataset used was acquired in 2018 as part of a research and development project conducted by the utility company Energisa. Data collection was carried out using the RIEGL VMX-450 MLS system, equipped with dual scanning sensors capable of capturing over one million measurements per second (RIEGL, 2015). The two urban areas previously described contain point cloud densities exceeding 2 million points/m<sup>2</sup>.

### 2.2 Processing

The MLS data was pre-processed using TerraScan software through a routine that included noise filtering, DTM modeling, and subsequent height calculation and registration as an additional feature for all points relative to the calculated ground surface. Finally, points located a few centimeters above the ground were excluded, effectively removing ground-level points. The resulting dataset is illustrated in Figure 2, which shows the MLS point cloud color-coded by height, with ground points excluded.

The decision-rule-based algorithm developed in this work was applied to the point cloud after ground points were removed. The

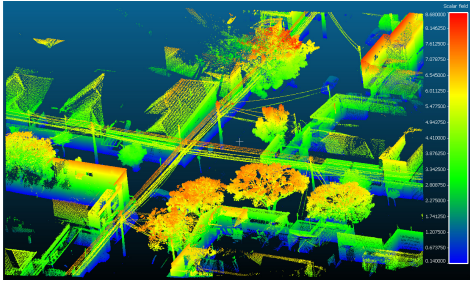


Figure 2. Height point values in Presidente Prudente downtown.

processing was parallelized into two pipelines: one dedicated to the power distribution networks components, and the other focused on tree detection. At the end of the process, the results were integrated to compute the touch distance between overhead cables and tree canopies. This distance was then assigned as an additional attribute to each detected tree object. The resulting information is highly valuable for vegetation management and pruning planning, as highlighted in the introductory section. Figure 3 presents an overview of the main workflow of the proposed processing pipeline.

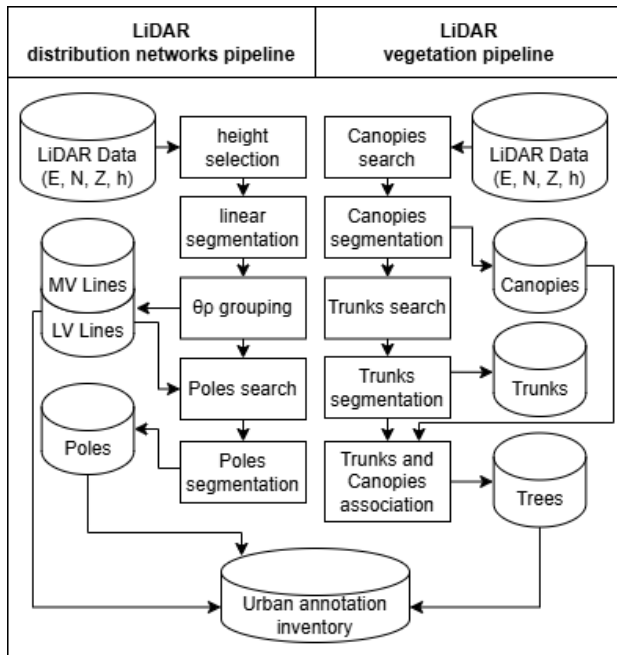


Figure 3. Proposed pipeline main workflow.

In the distribution network processing pipeline, the first step involves filtering the point cloud based on height intervals. Considering that LV and MV cables are installed at different heights according to ANEEL regulations, it is possible to define two distinct height ranges, one for each voltage level. By applying these filters, potentials points corresponding to each voltage level can be extracted, as illustrated in Figure 4.

After selecting the points based on height, the linearity tensor metric  $L$  for each point is computed through eigenvalue analysis (West et al., 2004), using the corresponding equating presented in Table 1.

The  $L$  values are constructed within a 3D Spherical Neighborhood that applies FLANN (Muja and Lowe, 2014) library around the points (3DSNF). With the linearity values computed for each point and for both height ranges (LV and MV

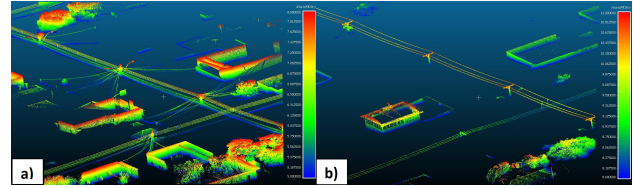


Figure 4. Low (a) and Medium (b) Voltage potential points after height selection.

Structure Tensor	Model
Linearity ( $L$ )	$(\lambda_1 - \lambda_2)/\lambda_1$
Sphericity ( $S$ )	$1 - ((\lambda_1 - \lambda_3)/\lambda_1)$

Table 1. Eigenvalues tensor metrics.

candidates), we obtain a visualization such as the one shown in Figure 5, where points corresponding to power cables are clearly highlighted. In the case of LV cables, an interesting characteristic emerges: the neighborhood radius must be set to less than 15 cm, as the spacing between the four conductors that make up the LV network typically ranges from 15 to 20 cm.

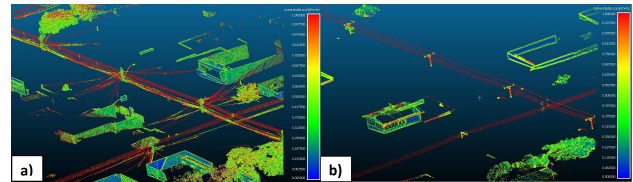


Figure 5. Linearity values in Low (a) and Medium (b) Voltage potential points.

The points are subsequently filtered again by retaining those with a threshold  $L_{th}$  obtained empirically that keeps high linearity values. Then, a segmentation algorithm based on region growing is applied to the remaining points, using a 3DSNF as the criterion for aggregating points that belong to the same object. The objective at this stage is to cluster points corresponding to power cables as well as residual noise that may still be present. These initial groupings are then further aggregated into larger segments through an analysis of proximity based on the  $\theta$  (theta) and  $\rho$  (rho) parameters, derived from the 2D Hough Transform (Duda and Hart, 1972) and Picture (Dudani and Luk, 1978).

At this point, most of the linear noise points that were still present in the selected data are filtered out, as they tend to cluster into small  $\theta$ - $\rho$  groups due to their limited spatial extent. In contrast, true conductors form larger, well-defined groups, typically extending over lengths of 15 m or more.

The results obtained after this stage — which processes the two voltage ranges (LV, MV) separately — are considered the annotation points for the Low and Medium Voltage cables classes. The pipeline then proceeds with the search for utility Poles. In this step, a 2D buffer is applied around the previously identified cables to constrain the search space (Figure 6a), limiting it to areas where pole-related points are likely to be found.

Within the defined buffer, a matrix is computed by summing the height values of all points contained in these regions (Sirmacek and Lindenbergh, 2015). The cells of this matrix containing the sum-height are then filtered, using an empirical threshold, to select only those likely to correspond to potential utility pole structures (Figure 6b).

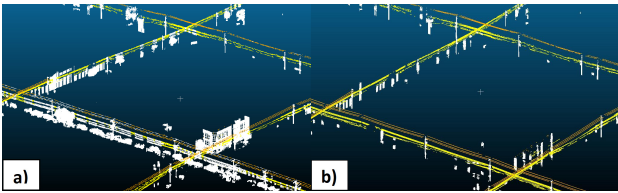


Figure 6. Points filtered by a 2D buffer around power cables (a) and after a maximum local sum-height filter (b).

Finally, the selected points are grouped through region growing using a 3DSNF. The resulting clusters are then filtered based on their overall height and linearity, effectively removing most of potential noise such as facade fragments or tree trunks. The results obtained can be represented separately from the rest of the point cloud, as shown in Figure 7.

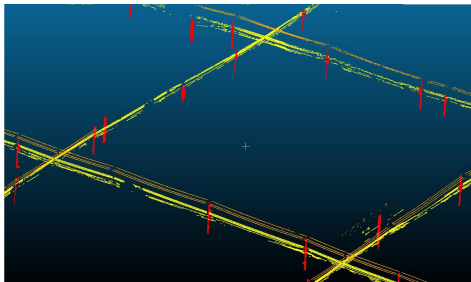


Figure 7. Points classified as Low Voltage cables (yellow), Medium Voltage cables (orange) and poles (red).

In the vegetation processing pipeline, the point cloud is voxelized with the aim of applying the sphericity tensor via eigenvalues (West et al., 2004) to the points inside each voxel representing the outermost leaf voxels, using  $S$  equation in Table 1 as well as the linearity for power cable points. The voxels are then filtered based on the empirically obtained sphericity threshold value  $S_{th}$  and the height of each voxel center, considering that voxels very close to the ground tend to correspond to shrubs and tall grass, and not necessarily tree canopies parts. The potential tree canopies points can be seen in Figure 8a. Subsequently, the voxels selected by sphericity are subjected to region growing considering the 3D neighborhood of the 26 adjacent voxels.

These voxel clusters are then evaluated using an internal decision-rule-based method that applies thresholds on point density. For each cluster, the total number of points within the grown voxels is considered. Clusters exceeding the first threshold, are automatically associated as a tree canopy candidate. Clusters below this threshold goes to a second and lower threshold, allowing a secondary selection of points after computing sphericity for all points in the cluster, rather than only within individual voxels (Figure 8b). More information related to this decision-rule method can be found in Oliveira (2022).

With the tree crowns delineated in the point cloud space, potential trunk points are selected using a 2D buffer beneath the identified crowns, constrained by a height threshold based on the lowest voxel of each cluster. These points are then grouped using a 3DSNF, aiming to model the various objects located beneath the trees. The resulting objects are subsequently filtered based on point density, eliminating small structures that represent noise beneath the crowns and were segmented during this process. The remaining objects are then considered as tree trunks and are associated with the crowns located above them, thereby forming the trees class in the annotation inventory. Some examples can be seen in Figure 9.

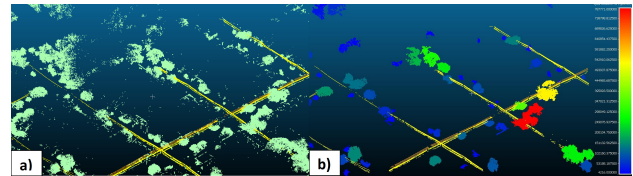


Figure 8. Potential canopies points (a) and canopies objects colored by points density (b).

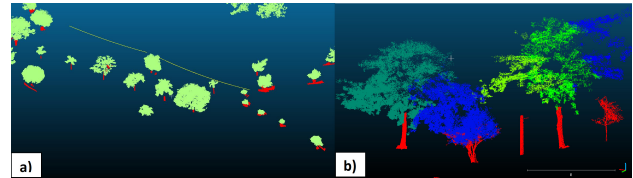


Figure 9. Trees canopies and trunks along a perspective zoom out view (a) and zoom in view (b).

### 2.3 Evaluation process

In this paper, for quality assessment, we used a publicly available dataset provided by the utility company Energisa, corresponding to the 2018 mobile LiDAR acquisition, to evaluate the proposed pipeline.

For power distribution networks, two approaches were employed to compute the quality metrics derived from the confusion matrix, both focused solely on distinguishing true positives (TP) from false positives (FP) and false negatives (FN), without considering confusion between different classes. The first evaluation approach computed quality metrics directly from the counting of network segments, which were defined as the intervals between consecutive poles along the power lines, as well as intervals between poles and the boundaries of the analyzed point cloud.

An example of how the network segments were counted is illustrated in Figure 10, which depicts the LV cables automatically generated by the proposed pipeline application and the reference LV segments provided by the utility company dataset. In this figure the red points indicate pole locations from the same reference database. Segments highlighted in pink represent examples of how reference segments are counted, including the cases where the segments are defined by the distance between a pole and the boundary of the analyzed cloud, rather than between two poles.

In this example, eight reference segments were identified. The algorithm-generated network successfully matched all eight segments from the reference, resulting in eight TPs. It is important to note that positional discrepancies between the modeled network and the reference were not considered in the evaluation. According to Brazilian regulations, ANEEL does not require utility companies to provide asset locations with absolute positional accuracy. Consequently, the databases supplied by the utilities often present spatial inaccuracies and other inconsistencies. Nevertheless, they remain suitable for use as a reference in comparative assessments.

The second approach calculated the quality metrics based on the total length of the identified network segments rather than segment counts. In this case, TPs and FPs were quantified by summing the lengths of correctly or incorrectly identified cable segments, respectively. FNs were measured as the cumulative

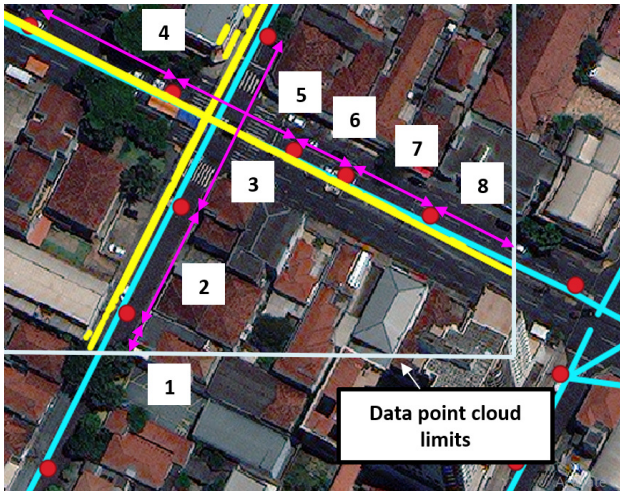


Figure 10. Example of LV segments comparison: reference (cyan) and pipeline results (yellow).

lengths of gaps where the algorithm failed to detect portions of the network present in the reference, whether these gaps occurred along parts of the segments or comprised entire segments

For pole evaluation, the detected pole points were compared to the reference database, considering a threshold of 4 m for association to be classified as a TP. It is important to highlight that no accuracy assessment was performed for the vegetation class. This decision was made because there was no available dataset or urban inventory providing a reliable reference for vegetation in the study area. Consequently, it was not possible to compute quality metrics or perform a comparative evaluation for this class.

### 3. Results and discussion

The decision-rule-based algorithm presented in this paper involves multiple parameters at each processing stage, which manage the progressive selection and filtering of points within the point cloud. Key geometric and empirical parameters include height ranges of 5 to 8 m and 8 to 11 m for LV and MV cable detection, respectively. The linearity metric employs a 3DSNF of 14 cm for LV and 50 cm for MV points, with  $L_{th}$  equal to 0.90. The  $\theta-\rho$  groups relies on parameters of  $4^\circ$  for  $\theta$  variation and 2 m for  $\rho$  variation, with a minimum linear segment length of 20 m for final modeling cables. Pole detection utilizes an empirically determined minimum height for maximum local sum height filter, and an object minimum height of 5.70 m to be considered as a true pole. In the vegetation pipeline, tree canopy voxel selection applies a minimum height of 1.10 m and  $S_{th}$  equal to 0.20, while leaf-voxels were created with a spatial resolution of 50 cm. Tree canopies selections and filtering parameters were related principally with the density of the potential targets and were also empirically set, consistently leveraging the 3DSNF for neighborhood computations.

A perspective detailed view can be seen in Figure 11, and an orthogonal view of the study regions is shown in Figure 12.

The results demonstrate that the decision-rule-based algorithm produces consistent and reliable outputs, especially excelling in the detection of electric components from the power distribution networks systems. The method accurately identifies both LV and MV cables, providing relevant spatial information for this

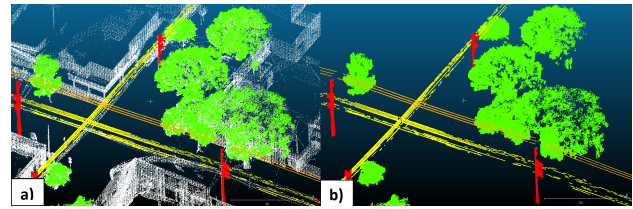


Figure 11. Example of a region classified into the four proposed classes: LV cables (yellow), MV cables (orange), poles (red) and trees (green), among the remaining points (a) and isolated (b).

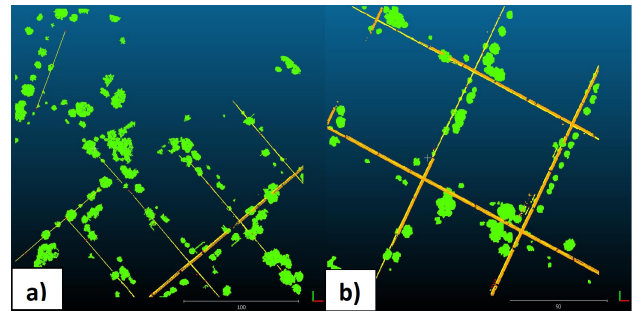


Figure 12. Orthogonal view of the classified cloud points obtained for the two regions presented in Figure 1.

utility management. Table 2 presents the quantitative measures obtained for components classification.

Class (approach)	Precision	Recall	F-Score
LV cables (1st approach)	0.933	0.897	0.915
LV cables (2nd approach)	0.966	0.886	0.924
MV cables (1st approach)	0.943	0.943	0.943
MV cables (2nd approach)	0.967	0.922	0.945
Poles	0.889	0.625	0.734

Table 2. Evaluation metrics for the test region.

Table 2 demonstrates how prioritizing the tuning of internal parameters within the pipeline contributed to achieving relatively good quality metrics for the electrical components. However, due to the inherent trade-off in parameter adjustment focusing on minimizing FPs, there is a consequent increase in FNs, negatively impacting the Recall metric. Most of the FN points for power lines are eventually associated with gaps caused by vegetation occlusion. For poles, the main limitation was the absence of a specific step capable of modeling building facades separately, considering that the parameter trade-off was adjusted to avoid confusion between poles and facade fragments. Nevertheless, since no quantitative metric was applied to assess vegetation, it is difficult to precisely measure whether the detection of this class yielded optimal results, even though, from a visual inspection, the method was able to accurately identify most of the relevant trees for the proposed pipeline.

### 4. Conclusions and future work

Despite the seemingly good results in the estimation of quality metrics and in the visual inspection, further actions can be taken to increase the reliability of the method. It is highly recommended that the method be tested in larger regions with greater variability or with another type of LiDAR sensor, adding other complex urban environments, with their own characteristics. Moreover, beyond the problems of

misclassification, the current approach has limitations, as it depends on setting certain parameters — many of which were not detailed in the previous section. This characteristic reduces the scalability of the solution when applied in real life data.

However, for the intended purpose of serving as an initial source for data annotation, the results are satisfactory. Since the goal is to use this output as annotated data, it is considered preferable to prioritize more precise detections rather than maximizing the number of detected objects, even if this leads to a proportional increase in FNs. To express it differently, Precision is considered more relevant than Recall when the main objective is to automatic feed data for annotation.

For future work, it is intended to reduce, as much as possible, the number of internal parameters required at each stage of the algorithm. Additionally, to improve the reliability of the vegetation-related results, a dedicated database of trees located near the power distribution networks will be developed. This database will serve as a reference for more accurate validation of this class. Furthermore, the ultimate goal is to use the annotated data generated in this process to train neural networks, enabling the evaluation and comparison of models trained with manually created annotations versus those trained with the primarily semi-automatic annotation proposed in this work.

### Acknowledgements

The authors would like to thank the support of Concert Technologies for manage with Energisa the project that collected the data and Energisa for providing it, the PPGCC - Graduate Program in Cartographic Sciences at Unesp - São Paulo State University, CAPES - Coordenação de Aperfeiçoamento de Pessoal de Nível Superior - Brasil, and CNPq - National Council for Scientific and Technological Development (grant n. 309735/2022-3).

### References

- Alaba, S. Y., Ball, J. E., 2022. A Survey on Deep-Learning-Based LiDAR 3D Object Detection for Autonomous Driving. *Sensors*, 22(24), 9577. <https://doi.org/10.3390/s22249577>.
- Alencar, C. J., Galo, M., Santos, R. C. d., 2023. Uso de Descritores 3D e Intensidade na Detecção de Árvores em Ambiente Urbano por meio de Dados LiDAR. *Revista Brasileira de Cartografia*, 75. <https://doi.org/10.14393/rbcv75n0a-63073>.
- ANEEL - Agência Nacional de Energia Elétrica, 2021. Anexo I da Resolução Normativa ANEEL nº 956, de 7 de dezembro de 2021: Procedimentos de Distribuição de Energia Elétrica no Sistema Elétrico Nacional – PRODIST. Módulo 1 – Glossário de Termos Técnicos do PRODIST. *Agência Nacional de Energia Elétrica (ANEEL)*. Published on December 7, 2021.
- Bergmann, M. A., Rodrigues Moreira, L. F., Krohling, B., Silveira, T. L. T., Jung, C. R., Tang, J., Feitosa, M. V., Gomes, R. L. B., Soares, B. N., 2024. An Approach Based on LiDAR and Spherical Images for Automated Vegetation Inspection in Urban Power Distribution Lines. *IEEE Access*, 12, 105119–105130. <https://doi.org/10.1109/ACCESS.2024.3431466>.
- Carvalho, F. B. S., Medeiros, T. I. O., Rodriguez, Y. P. M., 2018. Monitoring System for Vegetation Encroachment Detection in Power Lines Based on Wireless Sensor Networks. *2018 41st International Conference on Telecommunications and Signal Processing (TSP)*, 1–4. <https://doi.org/10.1109/TSP.2018.8441408>.
- Cerrai, D., Watson, P., Anagnostou, E. N., 2019. Assessing the effects of a vegetation management standard on distribution grid outage rates. *Electric Power Systems Research*, 175, 105909. <https://doi.org/10.1016/j.epr.2019.105909>.
- Chen, C., Yang, B., Song, S., Peng, X., Huang, R., 2018. Automatic Clearance Anomaly Detection for Transmission Line Corridors Utilizing UAV-Borne LIDAR Data. *Remote Sensing*, 10(4), 613. <https://doi.org/10.3390/rs10040613>.
- de Oliveira, R. A. R., 2022. Extraction of aerial electrical power distribution networks and identification of vegetation contact regions from data obtained by LASER scanning systems. *Institutional Repository of Universidade Estadual Paulista (UNESP)*, Master's Thesis(FCT - Presidente Prudente), 1–140. <http://hdl.handle.net/11449/244100>.
- dos Santos, R. C., Galo, M., Habib, A. F., 2022. K-Means Clustering Based On Omnivariance Attribute For Building Detection From Airborne LiDAR Data. *ISPRS Annals of the Photogrammetry, Remote Sensing and Spatial Information Sciences*, V-2-2022, 111–118. <https://doi.org/10.5194/isprs-annals-V-2-2022-111-2022>.
- Duda, R. O., Hart, P. E., 1972. Use of the Hough transformation to detect lines and curves in pictures. *Commun. ACM*, 15(1), 11–15. <https://doi.org/10.1145/361237.361242>.
- Dudani, S. A., Luk, A. L., 1978. Locating straight-line edge segments on outdoor scenes. *Pattern Recognition*, 10(3), 145–157. [https://doi.org/10.1016/0031-3203\(78\)90023-7](https://doi.org/10.1016/0031-3203(78)90023-7).
- Lehtomäki, M., Kukko, A., Matikainen, L., Hyypä, J., Kaartinen, H., Jaakkola, A., 2019. Power line mapping technique using all-terrain mobile laser scanning. *Automation in Construction*, 105, 102802. <https://doi.org/10.1016/j.autcon.2019.03.023>.
- Li, Y., Li, L., Li, D., Yang, F., Liu, Y., 2017. A Density-Based Clustering Method for Urban Scene Mobile Laser Scanning Data Segmentation. *Remote Sensing*, 9(4), 331. <https://doi.org/10.3390/rs9040331>.
- Matikainen, L., Lehtomäki, M., Ahokas, E., Hyypä, J., Karjalainen, M., Jaakkola, A., Kukko, A., Heinonen, T., 2016. Remote sensing methods for power line corridor surveys. *ISPRS Journal of Photogrammetry and Remote Sensing*, 119, 10–31. <https://doi.org/10.1016/j.isprsjprs.2016.04.011>.
- Muja, M., Lowe, D. G., 2014. Scalable Nearest Neighbor Algorithms for High Dimensional Data. *Pattern Analysis and Machine Intelligence, IEEE Transactions on*, 36. <https://doi.org/10.1109/TPAMI.2014.2321376>.
- Munir, N., Awrangjeb, M., Stantic, B., 2023. Power Line Extraction and Reconstruction Methods from Laser Scanning Data: A Literature Review. *Remote Sensing*, 15(4), 973. <https://doi.org/10.3390/rs15040973>.
- Sirmacek, B., Lindenbergh, R., 2015. Automatic Classification Of Trees From LASER Scanning Point Clouds. *ISPRS Annals of the Photogrammetry, Remote Sensing and Spatial Information Sciences*, II-3-W5, 137–144. <https://doi.org/10.5194/isprsannals-II-3-W5-137-2015>.

Wang, Y., Chen, Q., Zhu, Q., Liu, L., Li, C., Zheng, D., 2019. A Survey of Mobile Laser Scanning Applications and Key Techniques over Urban Areas. *Remote Sensing*, 11(13), 1540. <https://doi.org/10.3390/rs11131540>.

Wang, Y., Sun, P., Chu, W., Li, Y., Chen, Y., Lin, H., Dong, Z., Yang, B., He, C., 2024. Efficient multi-modal high-precision semantic segmentation from MLS point cloud without 3D annotation. *International Journal of Applied Earth Observation and Geoinformation*, 135, 104243. <https://doi.org/10.1016/j.jag.2024.104243>.

West, K. F., Webb, B. N., Lersch, J. R., Pothier, S., Triscari, J. M., Iverson, A. E., 2004. Context-driven automated target detection in 3D data. *Automatic Target Recognition XIV*, 5426, 133–143. <https://doi.org/10.1117/12.542536>.

Xiang, B., Yue, Y., Peters, T., Schindler, K., 2023. A Review of panoptic segmentation for mobile mapping point clouds. *ISPRS Journal of Photogrammetry and Remote Sensing*, 203, 373–391. <https://doi.org/10.1016/j.isprsjprs.2023.08.008>.

Zhang, R., Xue, Y., Wang, J., Song, D., Zhao, J., Pang, L., 2024. MSFA-Net: A Multiscale Feature Aggregation Network for Semantic Segmentation of Historical Building Point Clouds. *Buildings*, 14(5), 1285. <https://doi.org/10.3390/buildings14051285>.

Zhu, L., Hyypä, J., 2014. The Use of Airborne and Mobile Laser Scanning for Modeling Railway Environments in 3D. *Remote Sensing*, 6(4), 3075–3100. <https://doi.org/10.3390/rs6043075>.

Zou, X., Li, J., Wu, W., Liang, F., Yang, B., Dong, Z., 2025. Reliable-loc: Robust sequential LiDAR global localization in large-scale street scenes based on verifiable cues. *ISPRS Journal of Photogrammetry and Remote Sensing*, 224, 287–301. <https://doi.org/https://doi.org/10.1016/j.isprsjprs.2025.03.029>.